

A new anti-reflection surface structure for photonic crystal slab lens

B. Zhang^a and M.Y. Li

School of Electronics and Information Engineering, Beijing Jiaotong University, Beijing 100044, P.R. China

Received 11 May 2007 / Received in final form 5 July 2007

Published online 27 July 2007 – © EDP Sciences, Società Italiana di Fisica, Springer-Verlag 2007

Abstract. An optimized surface modification structure for suppressing the reflections at the surfaces of photonic crystal slab lens is reported in this paper. The total reflection of the slab lens with proposed anti-reflection surface structure is reduced to below 0.3% for the incident angle of light less than 48 degrees. The image efficiency of the slab lens for the normal incident Gaussian beam with waist width equal to the wavelength is near 99%.

PACS. 42.70.Qs Photonic bandgap materials – 42.25.Gy Edge and boundary effects; reflection and refraction – 78.68.+m Optical properties of surfaces

1 Introduction

The photonic crystal slab lens based on the negative refraction at the interface of air and photonic crystal have been intensely studied recently [1,2], and is a promising candidate to substitute the traditional curved surfaces lens in new generation of planar lightwave circuits. Nevertheless, the high reflection from the surfaces of lens is still main obstacle for widely putting the photonic crystal lens into practical application [3,4]. Some methods have been proposed for reducing the reflections at the interfaces of air and photonic crystal, and the simplest one uses the destructive interference of reflected rays at the two surfaces of the lens to get zero reflection [5]. Since this method is based on the interference, it is sensitive to the incidence angle of the incident rays, which limits the numerical aperture of the lens. Momeni et al. [6] proposed adiabatic matching stage to eliminate the reflection, resulting in nearly perfect transmission in a wide range of incident angle. However, the large size required for the adiabatic matching stage limits the range of its application. Recently, Sterke et al. [7] reported rod-type photonic crystals with quite low interface reflection in the ultra wide range of incidence angle, but since this property is limited to specific structure, it is not straightforward to apply it to all-angle negative refraction slab lens. Surface modification is a widely discussed method to eliminate the reflection from the interface between free space and photonic crystals [8], i.e. by changing the size or shape of the air holes, or adding an additional row of holes, the reflection can be suppressed to an acceptable level. However, the reported results are limited to small range of incidence

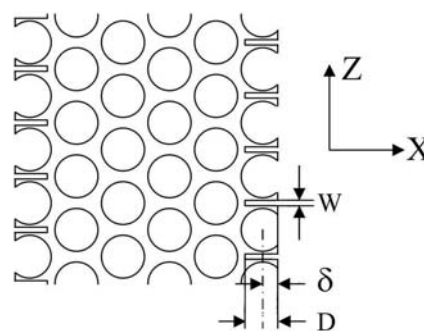


Fig. 1. Configuration of photonic crystal slab lens and anti-reflection surface structure.

angle. In this paper, it is presented that an optimized surface structure designed to the slab lens can reduce the total reflections of the lens to the level less than 0.3% for the incidence angle of light less than 48 degrees.

2 Structure and simulation results

We consider a two-dimensional triangular lattice of air-holes in a dielectric material with dielectric constant $\varepsilon = 11.96$ and $r = 0.4a$ for the E polarization (E field parallel to the axis of air holes), where r is the radius of the cylindrical air-holes and a is the lattice constant. The slab lens is consisted of six rows of air-holes as shown in Figure 1, where δ is the distance between the surface of the photonic crystal slab and the axes of outermost cylinder holes. In order to suppress the surface reflection of the slab lens, we cave slots at both surfaces of the slab in the middle of two outermost neighbor air-holes. The

^a e-mail: zhangb@center.njtu.edu.cn

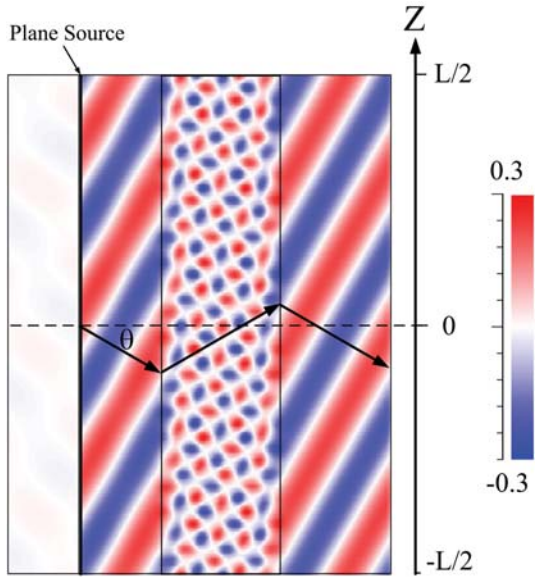


Fig. 2. (Color online) Electric field distribution for the slab lens with the optimized surface structure excited by plane wave source, where $L = 20a$ and $\theta = 29.937^\circ$.

width of the slots is $W = 0.1a$ and the depth is D . To ensure the all-angle negative refraction, we chose the frequency $\omega = 0.3006(2\pi c/a)$, at which the effective refractive index n_{eff} of the photonic crystal equates to -1 . We calculated the reflection coefficient of the slab lens using a two-dimensional finite-difference time-domain (FDTD) method with perfectly-matched layers boundary condition in horizontal direction and simplified periodic boundary condition in vertical direction. Here, we adjust the length of the simulation domain along vertical direction $L = Ma$ and incidence angle of light θ to satisfy the relation $L2\pi/\lambda \sin \theta = 2\pi N$, where λ is wavelength in vacuum and M, N are integer numbers, so that the periodical boundary condition $\psi(x, L/2) = \psi(x, -L/2) \exp(i2\pi/\lambda L \sin \theta)$ is simplified to $\psi(x, L/2) = \psi(x, -L/2)$. The spatial discretization value used here is $\Delta = 0.02a$.

The angular dependence of the reflection coefficient of the slab lens for excitation by a plane source located before the left surface of the slab is given by $R(\theta) = |P_x/P_0|$, where P_x is the power of reflection along the x -direction, P_0 is the power of incident plane wave along the x -direction. In order to reduce the reflection coefficient to a minimum over large incident angle range, we scan the parameters δ from $(-\sqrt{3}/4)a$ to $(\sqrt{3}/4)a$ and D from 0 to $(3\sqrt{3}/4 - 0.4)a$ with step value $0.02a$ and the result optimized configuration is $\delta = 0.22a$ and $D = 0.62a$. Figure 2 shows the electric field distribution for the slab lens with the optimized surface structure excited by oblique incident plane wave, where the width of simulating domain is $L = 20a$ and the incidence angle is $\theta = 29.937$ degrees. The total reflection of the slab lens is only 0.17%.

The result of numerical simulation for the angular dependence of the reflection coefficient of the slab lens with the optimized surface structure is presented in Figure 3. The reflection coefficient of left surface is also presented.

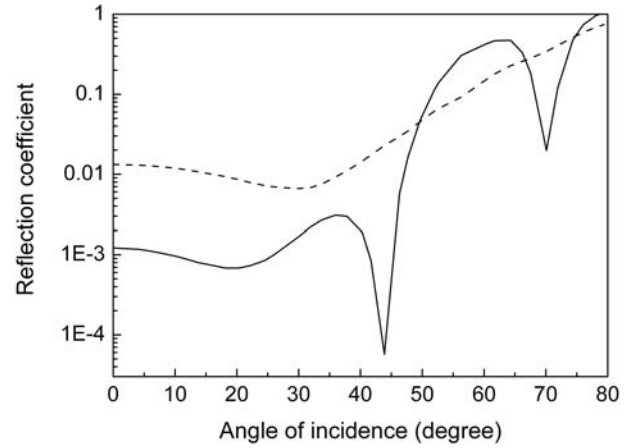


Fig. 3. Angular dependence of the reflection coefficient of slab lens (solid line) and left interface (dashed line) with optimized surface configuration $\delta = 0.22a$ and $D = 0.62a$.

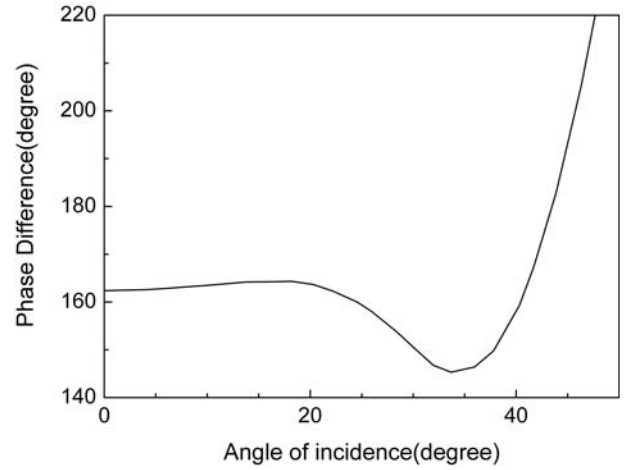


Fig. 4. Angular dependence of the phase difference between the rays reflected at the right interface and left interface of the slab lens.

As shown in Figure 3, the reflection from the surfaces of the slab lens is reduced to the level below 0.3% for the incident angle range $\theta < 48^\circ$. We notice that for that incident angle range, the reflection at the left interface is still of the order 1%, much higher than that of total reflection of the slab lens, indicating that weakening interference of the rays reflected at the two surfaces of the slab occurs.

To understand this feature, we calculate the phase difference between the rays reflected at the right and left surfaces of the slab lens vs. angle of incidence; the result is shown in Figure 4. In the angular range $\theta < 48^\circ$, the value of phase difference is between $180^\circ - 40^\circ$ to $180^\circ + 40^\circ$, resulting strong weakening interference. The phenomenon of large angular range for strong weakening interference may be related to the generalized Goos-Hänqen effect [9]: the incident beam is reflected or refracted at a plane different from the actual interface, introducing additional angular sensitive phase shift to the reflected rays.

The far field image characteristic of the lens is numerical simulated by FDTD method. Figure 5 shows the

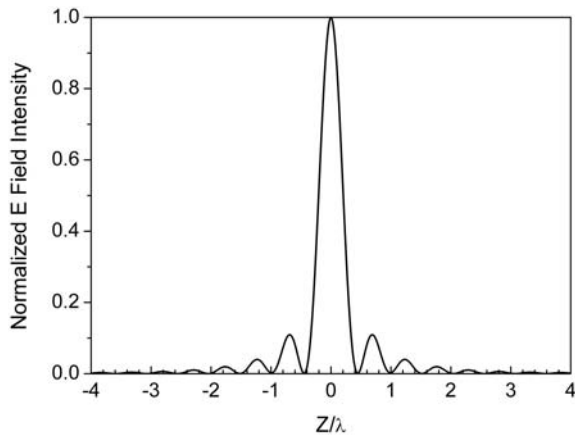


Fig. 5. The normalized electric field intensity across the image center, parallel to the surface of the lens.

normalized electric field intensity across the image center, parallel to the surface of the lens, produced by a line source placed to the left of the lens, located at the distance $u = a$ from left interface. We use the full width at half maximum (FWHM) of the image intensity to evaluate the image quality. We obtain the resolution of the lens is 0.412λ , which is slightly better than that of the lens without the anti-reflection surface structure [10]. We obtain the image efficiency of the slab lens for the line source $\eta = P_{0z}/P_{s+} = 0.726$, where P_{0z} is the power along z -direction within the main lobe at image plane and P_{s+} is the power of the source along positive z -direction.

We investigate the image properties of the slab lens for the normal incidence Gaussian beam using a two-dimensional FDTD method with perfectly-matched layers boundary condition. Figure 6 shows the electric field distribution across slab lens for Gaussian source. Where the waist width of the Gaussian beam equates the wavelength λ . The total reflection of the slab lens is only 0.24%. We obtain the image efficiency of the lens for the Gaussian beam $\eta = 98.7\%$, which is defined as the ratio of the power within the main lobe at image plane to the total power of the incidence Gaussian beam.

3 Conclusion

An optimized surface structure for suppressing the reflection of photonic crystal slab lens is reported in this paper, for the incident angle of light less than 48 degrees, the

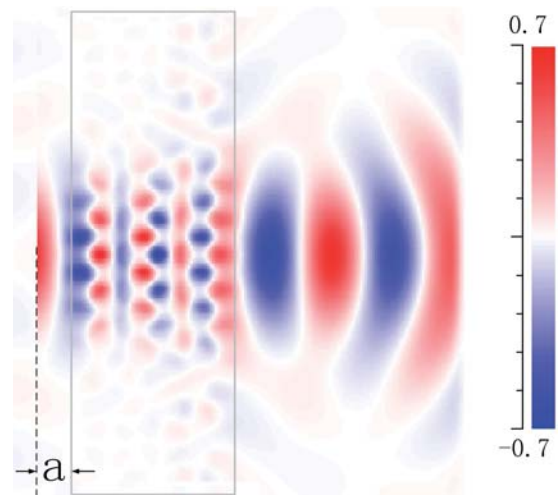


Fig. 6. (Color online) Electric field distribution for the slab lens with the optimized surface structure excited by normal incidence Gaussian beam. The waist of the beam is located at the distance $u = a$ from left interface.

reflection of the slab lens can be reduced to below 0.3%. The proposed anti-reflection surface structure is compact, and improves the image quality of the slab lens, especially fit for micromation.

References

1. J.B. Pendry, Phys. Rev. Lett. **85**, 3966 (2000)
2. M. Notomi, Phys. Rev. B **62**, 10696 (2000)
3. Z.C. Ruan, M. Qiu, S.S. Xiao, S.L. He, L. Thylén, Phys. Rev. B **71**, 045111 (2005)
4. S.S. Xiao, M. Qiu, Z.C. Ruan, S.L. He, Appl. Phys. Lett. **85**, 4269 (2004)
5. C.Y. Luo, S.G. Johnson, J.D. Joannopoulos, J.B. Pendry, Phys. Rev. B **65**, 201104 (2002)
6. B. Momeni, A. Adibi, Appl. Phys. Lett. **87**, 171104 (2005)
7. C.M. Sterke, T.P. White, Proc. SPIE **6128**, 61281B-1 (2006)
8. T. Baba, T. Matsumoto, M. Echizen, Opt. Expr. **12**, 4608 (2004)
9. D. Felbacq, R. Smaâli, Phys. Rev. Lett. **92**, 193902 (2004)
10. G. Sun, A.S. Jugessur, A.G. Kirk, Opt. Expr. **14**, 6755 (2006)